EXPERIMENTAL CELL RESEARCH 323 (2014) 87–99

Available online at www.sciencedirect.com

ScienceDirect

journal homepage: www.elsevier.com/locate/yexcr

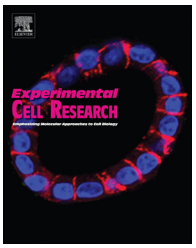

Research Article

A morphological and functional comparison of proximal tubule cell lines established from human urine and kidney tissue

J. Jansen[a,b,c,1], C.M.S. Schophuizen[a,b,c,1], M.J. Wilmer[a], S.H.M. Lahham[e], H.A.M. Mutsaers[a,b,c], J.F.M. Wetzels[d], R.A. Bank[e], L.P. van den Heuvel[c,f], J.G. Hoenderop[b], R. Masereeuw[a,*]

[a]Department of Pharmacology and Toxicology, Radboud University Medical Center, Nijmegen, The Netherlands
[b]Department of Physiology, Radboud University Medical Center, Nijmegen, The Netherlands
[c]Department of Pediatrics, Radboud University Medical Center, The Netherlands
[d]Department of Nephrology, Radboud University Medical Center, The Netherlands
[e]Department of Pathology and Medical Biology, University Medical Center Groningen, University of Groningen, Groningen, The Netherlands
[f]Department of Pediatrics, Catholic University Leuven, Leuven, Belgium

ARTICLE INFORMATION

Article Chronology:
Received 14 October 2013
Received in revised form
22 January 2014
Accepted 9 February 2014
Available online 18 February 2014

Keywords:
Bioartificial kidney
Regenerative nephrology
Transport
ECM

ABSTRACT

Promising renal replacement therapies include the development of a bioartificial kidney using functional human kidney cell models. In this study, human conditionally immortalized proximal tubular epithelial cell (ciPTEC) lines originating from kidney tissue (ciPTEC-T1 and ciPTEC-T2) were compared to ciPTEC previously isolated from urine (ciPTEC-U).

Subclones of all ciPTEC isolates formed tight cell layers on Transwell inserts as determined by transepithelial resistance, inulin diffusion, E-cadherin expression and immunocytochemisty. Extracellular matrix genes collagen I and -IV α1 were highly present in both kidney tissue derived matured cell lines ($p<0.001$) compared to matured ciPTEC-U, whereas matured ciPTEC-U showed a more pronounced fibronectin I and laminin 5 gene expression ($p<0.01$ and $p<0.05$, respectively). Expression of the influx carrier Organic Cation Transporter 2 (OCT-2), and the efflux pumps P-glycoprotein (P-gp), Multidrug Resistance Protein 4 (MRP4) and Breast Cancer Resistance Protein (BCRP) were confirmed in the three cell lines using real-time PCR and Western blotting. The activities of OCT-2 and P-gp were sensitive to specific inhibition in all models ($p<0.001$). The highest activity of MRP4 and BCRP was demonstrated in ciPTEC-U ($p<0.05$). Finally, active albumin reabsorption was highest in ciPTEC-T2 ($p<0.001$), while Na^+-dependent phosphate reabsorption was most abundant in ciPTEC-U ($p<0.01$).

In conclusion, ciPTEC established from human urine or kidney tissue display comparable functional PTEC specific transporters and physiological characteristics, providing ideal human tools for bioartificial kidney development.

*Correspondence to: Radboud University Medical Center (149), P.O. Box 9101, 6500 HB, Nijmegen, The Netherlands. Fax: +31 24 36 14214.
E-mail address: roos.masereeuw@radboudumc.nl (R. Masereeuw).
[1] Both authors contributed equally.

http://dx.doi.org/10.1016/j.yexcr.2014.02.011
0014-4827

Introduction

Worldwide, about 2 million people suffering from renal disorders are treated with hemo- or peritoneal dialysis and this number still increases. Main factors contributing to this increase are aging, an increased incidence of diabetes mellitus and hypertension [1–3]. Known limitations of the current dialysis methods as treatment modalities are related to the relatively poor clearance of protein-bound uremic retention solutes [4]. Up to now, a large number of compounds have been classified as uremic retention solutes [5] and their accumulation may have severe clinical implications, such as renal fibrosis, bone disorders, cardiovascular disease and mental disorders [6]. The preferred treatment of patients with end-stage renal disease (ESRD) is transplantation [7], which improves their quality of life and substantially reduces costs associated with extended dialysis [8]. However, a tremendous shortage of donor organs as well as complications arising from immunosuppressive treatment and organ rejection after transplantation are profound problems worldwide [9–11].

To replace kidney function, tissue engineering is a promising avenue of research to overcome the limitations of currently available renal replacement therapies [12]. The development of functional and stable human renal epithelial cell models that are able to actively excrete uremic retention solutes, is a promising step towards a bioartificial kidney device. In the kidney, a heterogeneous cell system is present of which the proximal tubular epithelial cells (PTEC) play an important role in the excretion of endo- and xenobiotics, including uremic retention solutes. The excretory pathway is mediated via a complex interplay involving solute carriers, like OCT-2 (*SLC22A2*), OAT-1 (*SLC22A6*) and OAT-3 (*SLC22A8*) [13], and ATP-binding cassette efflux pumps, such as p-glycoprotein; P-gp (*ABCB1*), MRP4 (*ABCC4*) and BCRP (*ABCG2*) [14]. Besides waste product excretion, reabsorption of filtered solutes, such as phosphate, glucose, urate and albumin, occurs in PTEC [15–18].

In our group, a stable PTEC cell line isolated from human urine was developed (ciPTEC-U) [19]. This cell line demonstrated functional characteristics of important in- and efflux transporters as well as active albumin and sodium-dependent phosphate transport [19], and has proven to be valuable in elucidating renal pathological mechanisms [20–23] and in studying renal physiological transport pathways [24–26]. However, as this cell line originates from urine, it could be argued that ciPTEC-U might not reflect the physiological situation as close as cells directly derived from kidney tissue. Cells originating from urine are often thought to be exfoliated from tissue due to apoptosis-induced loss of function [27]. Recently it was shown that overcrowding of epithelial cells due to proliferation and migration, induces the extrusion of living cells to maintain homeostasis in epithelial cell numbers [28]. The aim of this study was to compare ciPTEC-U [19] with newly established human proximal tubular epithelial cell lines from human kidney tissue with respect to important functional properties. Human PTEC were isolated from nephrectomised kidneys followed by subcloning and immortalization techniques. Characterizing the newly established human proximal tubular epithelial cell lines will allow us to determine whether the sample source influences renal functional properties of cell lines in culture. Insights in these characteristics allows to identify the most suitable cell line for further development of a bioartificial kidney device.

Materials and methods

Chemicals and cell culture materials

All chemicals were purchased from Sigma-Aldrich (Zwijndrecht, The Netherlands) unless stated otherwise. Cell culture plates were purchased from Greiner Bio-One (Monroe, NC) and Transwell inserts were obtained from Corning Costar (cat. no 3460, New York, NY).

Ethics statement

The kidney tissue used for cell line development in this study was obtained from non-transplanted donors, after given informed consent. These organs could not be transplanted due to quality loss of the veins during surgery. No clinical history of renal disorders or any other chronic disease were identified.

Isolation and culture of ciPTEC from kidney tissue

Purification and isolation of renal epithelial cells from kidney tissue was performed as described previously [29]. In short, epithelial cells were isolated by a gradient sieving procedure and subjected to collagenase digestion [30]. The collected primary fraction was transferred to supplemented PTEC culture media: phenol-red free DMEM-HAM's F12 medium (catalogue number 11039, Lonza, Basel, Switzerland) containing 10% (v/v) FCS (Greiner Bio-One, Monroe, NC), 5 μg/ml insulin, 5 μg/ml transferrin, 5 ng/ml selenium, 36 ng/ml hydrocortisone, 10 ng/ml EGF and 40 pg/ml tri-iodothyronine. Primary cells were immortalized within the first two passages. Immortalization was performed using a combination of hTERT and SV40t as described previously [19,31]. To obtain a homogeneous culture, cells were subcloned using irradiated NIH 3T3 fibroblast as non-dividing feeder cells [31]. After culturing for 2 weeks at 33 °C, 5% (v/v) CO_2, single cell clones were visible and picked using cloning discs drained in trypsin-EDTA (MP Biomedicals, Solon, OH). Single cell clones were transferred to a well plate and grown until confluency at 33 °C, 5% (v/v) CO_2. Optimal seeding conditions were determined for each obtained ciPTEC line in well plates and Transwell inserts (50 μg/ml collagen IV coating for ciPTEC-U (C6745-1 ml)) by testing morphological characteristics and monolayer integrity properties using a cell density range (data not shown). According to the conditions described previously [19], ciPTEC were cultured for 24 h at 33 °C 5% (v/v) CO_2 to proliferate and subsequently transferred to 37 °C, 5% (v/v) CO_2 for 7 days to mature. Up to at least 40 cell passage numbers were used to investigate proliferation and functional properties following prolonged culturing. Phase contrast images were captured using a Leica DM IL phase contrast microscope.

Immunocytochemistry

To investigate morphology and polarization characteristics of the ciPTEC monolayers, immunocytochemistry was performed using cells cultured on polyester Transwell inserts. Matured ciPTEC were fixed using 2% (w/v) paraformaldehyde in HBSS supplemented with 2% (w/v) sucrose for 5 min and permeabilized in 0.3% (v/v) triton X-100 in HBSS for 10 min. To prevent non-specific binding of

antibodies, cells were exposed to block solution containing 2% (w/v) bovine serum albumin fraction V (Roche, Woerden, The Netherlands) and 0.1% (v/v) tween-20 in HBSS for 30 min. Cells were incubated with antibodies diluted in block solution against the tight junction protein zonula occludens 1 (ZO-1, 1:50 dilution, Invitrogen, Carlsbad, CA) for 1 h, followed by incubation with goat-anti-rabbit-Alexa488 conjugate (1:200, Life Technologies Europe BV, Bleiswijk, The Netherlands) for 30 min. Finally, DAPI nuclei staining (300 nM, Life Technologies Europe BV) was performed for 5 min. Protein expression and localization were examined using the Olympus FV1000 Confocal Laser Scanning Microscope (Olympus, Tokyo, Japan) and images were captured using the Olympus software FV10-ASW version 1.7. Next, cell size measurements were performed using Image J software (version 1.40g).

Transepithelial barrier functions

Transepithelial resistance of matured ciPTEC monolayers on Transwell inserts was measured using the Millicell electrical resistance volt-ohm system (Millipore, Billerca, MA). Measurements were performed as described in the manufacturer's protocol. To determine the tightness of the ciPTEC monolayers, inulin–FITC (Sigma-Aldrich) diffusion was measured of matured ciPTEC cultured on Transwell inserts. Both apical and basolateral compartments were washed once with HBSS buffer (Life Technologies Europe BV), prior to 0.1 mg/ml inulin–FITC in HBSS basolateral exposure for 1 h at 37 °C, 5% (v/v) CO_2. Fluorescence was detected by measuring samples (200 µl) at excitation wavelength 485 nm and emission wavelength 535 nm, using a CytoFluor II Microplate reader (MTX Lab Systems, Vienna, VA).

To investigate monolayer development further, the presence of E-cadherin, a calcium-dependent cell–cell adhesion protein abundantly expressed in PTEC cells [32], was investigated in proliferating and matured cells. After harvesting, cells were fixed and permeabilized using 4% (w/v) PFA and 0.1% (v/v) saponin in HBSS on ice for 10 min. After centrifuging, cell pellets were resuspended in rat anti-E-cadherin antibody (1:100 in HBSS) and incubated at rT for 30 min. Next, cells were centrifuged again and pellets were resuspended in goat anti-rat Alexa 488 conjugate (1:200, Life Technologies Europe BV, Bleiswijk, The Netherlands) and incubated at rT for 30 min. After a final centrifuge step, cells were resuspended in HBSS buffer and measured using a flowcytometer (FACSCalibur BD, software BD CellQuest Pro version 6.0, Becton Dickinson, Franklin Lakes, NJ) gating on live cells (a total of 15,000 cells counted). Separate cell fractions were incubated solely with goat anti-rat Alexa 488 conjugate and signal measured was set as a negative control. Next to the extracted geometric mean data, representative flowcytometer histograms are shown to illustrate signal intensities (Alexa 488/FL1 signal).

Gene expression of relevant transporters and extracellular matrix proteins in ciPTEC

Total RNA was isolated from proliferating and matured cells using TRIzol (Life Technologies Europe BV) and chloroform extraction according to the manufacturer's protocol. The Omniscript RT kit (Qiagen, Venlo, The Netherlands) was used to synthesize cDNA. The mRNA expression levels of PTEC transporter genes were detected using gene specific primer-probe sets (Table S1, Applied Biosystems, CA, USA) and TaqMan Universal PCR Master Mix (Applied Biosystems). The quantitative PCR reactions were performed using the CFX96 Real Time PCR system (Bio-Rad Laboratories, Veenendaal, The Netherlands) and data were analyzed using the CFX Manager software (Bio-Rad Laboratories). The mRNA expression levels of extracellular matrix (ECM) genes were investigated using primer sets (Table S2) and SybrGreen PCR Master Mix (Qiagen). The quantitative PCR reactions were performed using the ABI 7900HT sequence detection system (Applied Biosystems, Nieuwekerk a/d IJssel, The Netherlands). Data of matured cells were normalized to expression levels of the reference gene GAPDH, and were expressed as fold increase compared to matured ciPTEC-U [19]. To compare expression levels from the proliferating towards matured stage per cell line, data of matured cells were expressed as fold increase compared to the corresponding proliferating cells (Supplementary Figs. S1 and S2).

Determination of proximal tubular specific transporter proteins

To detect proteins of interest in proliferating and matured cells, membrane fractions were obtained by ultracentrifugation. Confluent cell layers cultured in T175 flasks were harvested and homogenized in 30 ml buffer containing 18 mM Tris–HCl (pH 7.4), 6 mM EGTA, 0.3 M mannitol and protease inhibitors (100 mM phenylmethane sulphonylfluoride, 5 mg/ml aprotinin, 5 mg/ml leupeptin, and 5 mg/ml pepstatin). The suspension was homogenized using a tight fitting Dounce homogenizer (Kimble Chase LLC, Vineland, NJ) followed by ultracentrifugation (Sorval WX80, Thermo Fisher Scientific, Walhtam, MA) at 100,000*g* for 45 min at 4 °C. Finally, the membrane pellets were resuspended in 100 µl RIPA buffer containing 1% (w/v) Igepal CA630, 0.5% (w/v) Na-deoxycholate, 0.1% (v/v) SDS (Amersham Biosciences, NJ, USA) and protease inhibitors (0.01% (v/v) phenylmethane sulphonylfluoride, 3% (v/v) aprotinin and 1 mM sodium orthovanadate). The amount of total protein was measured using the Bio-Rad protein detection reagent system (Bio-Rad Laboratories). Protein expression of Organic Cation Transporter 2 (OCT-2), P-glycoprotein (P-gp), Multidrug Resistance Protein 4 (MRP4) and Breast Cancer Resistance Protein (BCRP) was investigated by Western blotting using 12%, 6%, 6% and 10% (w/v) sodium dodecyl sulfate polyacrylamide gel electrophoresis (SDS-PAGE), respectively. The iBlot Dry Blotting System (Life Technologies Europe BV) was used for transferring proteins from the gels onto a nitrocellulose membrane. To prevent non-specific binding of antibodies, membranes were blocked in PBS supplemented with 0.1% (v/v) tween-20 (PBS-T) and 5% (w/v) milk powder (Campina, Woerden, The Netherlands) for 30 min. Subsequently, membranes were washed three times in PBS-T. Next, membranes were incubated for 1.5 h with rabbit anti-OCT-2 antibody (1:500, Alpha Diagnostic International, San Antonio, TX), mouse anti-P-gp antibody (1:200, Abcam, Cambridge, UK), rabbit anti-MRP4 antibody (1:100, M49, [33]) or mouse anti-BCRP (1:200, Abcam®, Cambridge, UK). As a loading control mouse anti-β-actin (1:100,000) or rabbit anti-Na,K-ATPase antibody (α-subunit, 1:2,000, C356-M09 [34]) was used. Subsequently, after three washing steps in PBS-T, membranes were exposed to secondary antibodies Alexa fluor® 680 goat anti-rabbit IgG (1:10,000, Life Technologies Europe BV), IRDye 800 goat anti-mouse IgG (1:10,000, Rockland, PA) or IRDye 800 goat anti-rabbit IgG (1:10,000, Rockland, PA) for 1.5 h. Fluorescence was quantified using the Odyssey Infrared Imaging System (version 2.1, LICOR® Biosciences, Lincoln, NE). Data of proliferating and matured

cells were normalized to protein expression levels of the loading control and plotted in absolute pixel intensities.

Transport assays of renal in- and efflux proteins

The activity of the renal OCT influx proteins was measured as previously described by Schophuizen et al. [26]. In short, harvested matured cell suspensions were exposed to the fluorescent OCT substrate 4-(4-(dimethylamino)styryl)-N-methylpyridinium iodide (ASP^+) in the presence or absence of 5 mM OCT inhibitor tetrapentylammonium chloride (TPA). Data plotted were corrected for cell numbers.

The activity of the renal efflux protein P-gp in ciPTEC was examined by measuring the amount of calcein accumulation [35]. In short, matured cells were exposed to 1 μM calcein-AM (Life Technologies Europe BV) in the presence or absence of 5 μM P-gp inhibitor PSC833 (Tocris Biosciences, Bristol, UK) for 1 h at 37 °C, 5% (v/v) CO_2. Fluorescence in lysed cells was measured and data plotted were corrected for protein concentrations.

To evaluate transport characteristics of the renal efflux transporters BCRP and MRP4 [33,36], ciPTEC were exposed to kynurenic acid, the end product of tryptophan metabolism. Kynurenic acid is a known uremic retention solute and a substrate for both renal efflux transporters [24,25]. To investigate the transport properties of these proteins, cells were cultured in 24 well plates and matured monolayers were gently washed three times using Krebs–Henseleit buffer supplemented with 10 mM Hepes (pH 7.4, adjusted with Tris–HCl). Subsequently, cells were pre-incubated with supplemented Krebs–Henseleit buffer in the presence or absence of 5 μM KO143, a known BCRP inhibitor [37], and 5 μM MK 571 a known MRP inhibitor [38] (Alexis Biochemicals, Leiden, The Netherlands) at 37 °C, 5% (v/v) CO_2 for 2 h. After pre-incubation, cells were exposed to 10 μM ^{3}H-kynurenic acid (Scopus Research BV, Wageningen, The Netherlands) at 37 °C for 2 h. The uptake was terminated by washing the cells 3 times with ice-cold supplemented Krebs–Henseleit buffer. Cells were lysed using 0.1% (v/v) triton X-100. To each sample 2 ml of scintillation liquid was added and radioactivity was detected using liquid scintillation counting. Counts measured in supplemented Krebs–Henseleit buffer (blank) were subtracted and data plotted were corrected for protein concentrations.

Albumin and phosphate uptake assays

To investigate albumin uptake mediated by endocytosis, matured ciPTEC were exposed to serum free medium for 4 h at 37 °C, 5% (v/v) CO_2. Subsequently, cells were exposed to 50 μg/ml BSA–FITC and incubated at 37 °C, 5% (v/v) CO_2 for 30 min. In addition, experiments were performed at 4 °C to inhibit endocytosis. After the incubation period, cells were harvested and centrifuged at 1500*g* for 5 min. The cell pellet was resuspended in 4% (w/v) paraformaldehyde in PBS. Finally, intracellular albumin was measured using a flowcytometer (FACSCalibur BD, software BD CellQuest Pro version 6.0, Becton Dickinson, Franklin Lakes, NJ) gating on live cells (15,000 cells counted). Data was analyzed using FlowJo software (version 9.2) and relative net uptake data was plotted next to the actual flowcytometer histograms.

Phosphate uptake was performed in confluent monolayers cultured at 33 °C and 37 °C, 5% (v/v) CO_2 with $^{32}PO_4$ (Perkin Elmer, Waltham, MA) as described earlier by Malmstrom et al. [19,39]. Cells were cultured in 24 well plates and gently washed three times using wash buffer (20 mM Hepes, 5.6 mM $CaCl_2$, 10.8 mM KCl, 2.4 mM $MgCl_2$, 274 mM NaCl) at 37 °C. To determine the sodium-dependent uptake of phosphate, experiments were performed in the absence of sodium by replacing NaCl with 274 mM N-methyl-D-glucamine. The uptake buffer was added for 5 min at 37 °C consisting of wash buffer, supplemented with 0.22 mM phosphate with 1.0 μCi/mL $^{32}PO_4$ added as tracer. The uptake was terminated by washing the cells five times with ice-cold wash buffer. Cells were lysed using 0.5 ml 0.05 M Na^+-deoxycholate in 0.1 M NaOH. To each sample 2 ml of scintillation liquid was added and radioactivity was detected using liquid scintillation counting. Counts measured in wash buffer (blank) were subtracted and data plotted were corrected for protein concentrations.

Data analysis

All data are expressed as mean ± S.E.M. Statistical analysis was performed using one-way ANOVA analysis followed by Dunnett's Multiple Comparison test or, where appropriate, an unpaired *t* test with GraphPad Prism version 5.02 (La Jolla, CA). A *p*-value of <0.05 was considered significant.

Results

Successful development of ciPTEC lines from human kidney tissue isolates

To appreciate the functional capacity of ciPTEC-U [19], new PTEC cell lines were generated from human kidney tissue and characterized to compare with ciPTEC-U. PTEC isolates were obtained from three different kidney donors and primary cells were grown successfully. All cell cultures that were immortalized using SV40t and hTERT, were found resistant to both hygromycin B and geneticin (G418) thereby confirming successful transduction. Next, cells were subcloned to obtain homogenous cell lines after which cell proliferation could be maintained for up to at least cell passage 42 without morphological changes. From the original three kidney isolates, different subclones were obtained. Based on mRNA expression levels of PTEC transporters, morphology and monolayer tightness, two out of twenty six kidney subclones were selected (ciPTEC-T1 and -T2) for detailed characterization. The ciPTEC-T1 and -T2 originated from the same donor and were compared in great detail with ciPTEC-U [19]. Fig. 1a represents a flow chart of the isolation and selection procedure performed in this study. Representative phase contrast images of the selected clones ciPTEC-T1 and -T2 are shown in Fig. 1b. Transduction of kidney tissue derived cultures with hTERT solely did not result in suitable cell lines as determined by morphology and cell proliferation (data not shown).

Morphological characteristics and extracellular matrix investigation

Optimal seeding conditions to obtain confluent layers of ciPTEC in well plates and Transwell inserts were determined as indicated in Table 1. A collagen IV coating of 50 μg/ml stimulated the development of a homogeneous tight layer of ciPTEC-U on Transwell inserts. Interestingly, no coating was necessary for ciPTEC-T1 and

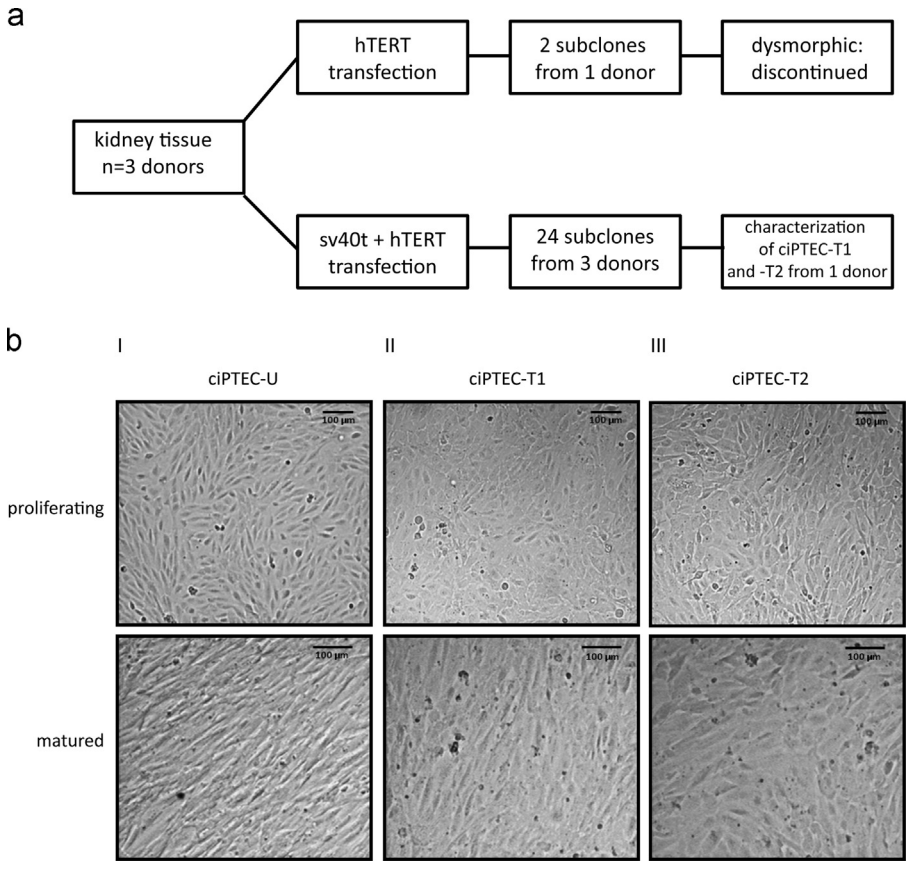

Fig. 1 – (a) Flow chart of clone selection. Schematic overview of the cell isolation process from kidney tissue upon establishment of clonal cell lines. Cells were isolated from three donors and 26 subclones were selected in a first round. These subclones were characterized morphologically, but also gene expression levels of PTEC specific transporters were investigated. Transduction of kidney tissue derived cultures with hTERT solely did not result in suitable cell lines as determined by morphology and cell proliferation. Finally, two clones from the same donor obtained after combined SV40 and hTERT transductions were chosen for detailed characterization (ciPTEC-T1 and -T2), based on PTEC specific morphological characteristics and highest gene expression levels of PTEC transporters. (b) Representative phase contrast images of ciPTEC. Proliferating (33 °C, 5% (v/v) CO_2) and fully matured (7 days at 37 °C, 5% (v/v) CO_2) ciPTEC-U passage 40 (I), -T1 passage 38 (II), and -T2 passage 42 (III) are shown.

Table 1 – Optimal ciPTEC seeding density in well plates and Transwell inserts.

Cell line	Well plates seeding density (cells · cm^{-2})	Transwell inserts seeding density (cells · cm^{-2})
ciPTEC-U	4.8×10^4	1.3×10^5
ciPTEC-T1	1.9×10^4	0.6×10^5
ciPTEC-T2	1.9×10^4	0.6×10^5

ciPTEC cultured at indicated densities resulted in tight monolayer formation upon 7 days maturation.

-T2 to develop a homogeneous cell monolayer on the inserts (Fig. 2a–c). In well plates, confluent ciPTEC monolayers were obtained without any additional coatings.

The tight junction protein zonula occludens-1 (ZO-1) in PTEC is a marker for the integrity and polarity of the cell layer. Furthermore, tight junctions contain interacting proteins that regulate differentiation, proliferation and gene expression, indicating an important role in PTEC functionality [40]. Cells cultured on Transwell inserts, were stained against ZO-1 and the protein expression was examined using confocal microscopy. A clear ZO-1 expression was visible for all three cell lines (Fig. 2a–c). A *z*-scan depicts the fluorescent signal of tight junction expression at the cell boundaries in each ciPTEC model, but most abundantly in ciPTEC-U, and confirms polarization of the cells. Next to this, we determined cell diameter and observed a larger span for matured ciPTEC-T1 (19.4 µm ± 0.8, $p < 0.001$; Fig. 2b) and -T2 (21.7 µm ± 0.6, $p < 0.001$; Fig. 2c) as compared to matured ciPTEC-U (10.9 µm ± 0.6; Fig. 2a). Both ciPTEC cell lines isolated from kidney tissue showed a larger span compared to ciPTEC-U when cultured in similar uncoated cell culture flasks, at both temperatures (Fig. 1b). This indicates that cell size differences were not influenced by a collagen IV coating but may possibly be source related.

Cell monolayer tightness was examined further by determination of the paracellular permeability of the cell monolayers using the diffusion marker inulin [41]. ciPTEC cultured on Transwell inserts were basolaterally exposed to inulin-FITC. No differences were observed in inulin flux between the ciPTEC-U versus kidney tissue derived cell lines, as shown in Table 2. Furthermore, the epithelial

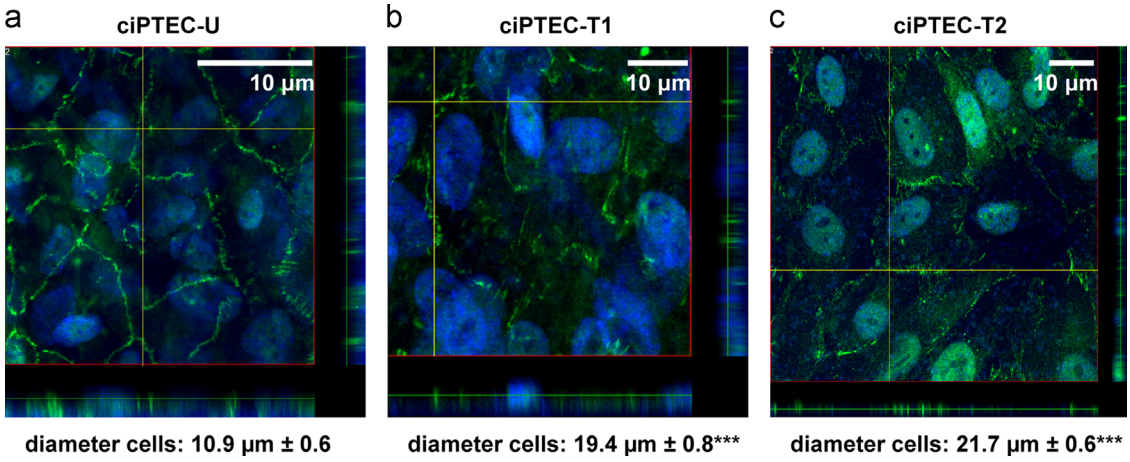

Fig. 2 – Expression of ZO-1 protein in ciPTEC. Representative confocal images of ZO-1 (green) in the *x–y* and *y–z* planes are shown (nuclei are stained with DAPI (blue)) in matured (37 °C) ciPTEC cultured on Transwell inserts. (a–c) The expression of ZO-1 (green fluorescent) was determined at the cell boundaries and was most abundantly present in ciPTEC-U (a). Furthermore, the average cell diameter was measured, demonstrating a significantly larger cell size of ciPTEC-T1 and -T2 as compared to ciPTEC-U. Note: ciPTEC-U were cultured on collagen IV coated surfaces, whereas ciPTEC-T1 and -T2 were cultured on uncoated Transwell inserts. *** = $p < 0.001$, using one-way ANOVA analysis followed by Dunnett's multiple comparison test.

barrier integrity was investigated by measuring the transepithelial electric resistance (TEER). Cell lines were cultured on Transwell inserts and the TEER was measured in matured cells (Table 2). CiPTEC-T1 demonstrated a higher resistance ($140 \pm 4\ \Omega/cm^2$, $p < 0.05$) as compared to ciPTEC-U ($124 \pm 3\ \Omega / cm^2$), whereas no significant differences were observed between ciPTEC-T2 ($126 \pm 4\ \Omega/cm^2$) and ciPTEC-U.

The cell–cell adhesion protein E-cadherin was clearly present in the models tested (Fig. 3) in proliferating (light gray histogram) as well as in matured (dark gray histogram) ciPTEC compared to the negative control (black histogram), emphasizing the abundant epithelial characteristics of these models. Interestingly, matured ciPTEC showed a more heterogeneous population compared to proliferating ciPTEC. Based on geometric mean data extracted from these histograms, only matured ciPTEC-T1 showed a more abundant prevalence of E-cadherin when compared to proliferating ciPTEC-T1.

To gain more insight in complexes involved in cell development [42,43], the presence of ECM genes was investigated. The mRNA expression levels of collagen I and –IV αI, fibronectin I and laminin 5 (LAMA5; alpha-5 subunit of laminin-10, -11 and -15) were detected in matured ciPTEC-U, -T1 and -T2. Interestingly, significant differences were observed between the cell lines. In matured ciPTEC-T1 and -T2 a higher expression of collagen I – and IV αI (Fig. 4a and b, $p < 0.001$) was observed compared to matured ciPTEC-U. Whereas fibronectin I and laminin 5 expression was lower in matured kidney tissue derived cell lines (fibronectin I ciPTEC-T1 and -T2: $p < 0.01$, laminin 5 ciPTEC-T2: $p < 0.05$, ciPTEC-T1: not significant) compared to ciPTEC-U. In Supplementary Fig. S1, mRNA expression levels of these genes in proliferating versus matured cells are shown. Matured tissue derived cell lines showed an increased collagen I αI (Fig. S1a; $p < 0.001$), fibronectin I (Fig. S1c; $p < 0.001$) and laminin 5 (Fig. S1d; $p < 0.05$) gene expression, whereas matured ciPTEC-U showed a less pronounced genetic ECM profile. Interestingly, collagen IV αI (Fig. S1b) gene expression upon maturation was lower ($p < 0.001$) in each cell line compared to proliferating cells.

Table 2 – Transepithelial barrier functions of ciPTEC.

Cell line	Inulin diffusion ($pmol \cdot min^{-1} \cdot cm^{-2}$)	TEER (Ω/cm^2)
ciPTEC-U	9.3 ± 0.4	124 ± 3
ciPTEC-T1	8.0 ± 0.7	140 ± 4*
ciPTEC-T2	9.2 ± 0.5	126 ± 4

Monolayer integrity was measured using inulin flux and transepithelial electric resistance determination.
* $p < 0.05$, using one-way ANOVA analysis followed by Dunnett's multiple comparison test. Data presented are means of three independent experiments and expressed as mean ± S.E.M.

Gene and protein expression levels of PTEC specific transporters

The excretion of endo- and xenobiotics in the proximal tubular system is mediated via various important in- and efflux transporters like OCT-2, P-gp, MRP4 and BCRP [13,14]. The presence of these PTEC specific transporters was investigated on gene and protein level in matured ciPTEC-U, -T1 and -T2. The mRNA expression levels of most transporters (Fig. 5) were comparable between the three matured cell lines, except for OCT-2 in ciPTEC-T1 ($p < 0.05$) and BCRP in ciPTEC-T2 ($p < 0.05$) which showed a higher expression as compared to matured ciPTEC-U. In Supplementary Fig. S2, mRNA expression levels of these genes in proliferating versus matured cells are shown. Each matured cell line showed an increased OCT-2 gene expression (Fig. S2a; ciPTEC-U and -T1 $p < 0.05$, ciPTEC-T2 $p < 0.001$), whereas P-gp (Fig. S2b) and MRP4 (Fig. S2c) gene expressions were more abundant only in matured tissue-derived cell lines (P-gp ciPTEC-T1 $p < 0.01$, ciPTEC-T2 $p < 0.05$; MRP4 ciPTEC-T2 $p < 0.01$). Although not significant, the gene expression of BCRP (Fig. S2d) showed less expression upon maturation in each cell line.

In fully differentiated cells, a non-significant but recurrent trend in abundancy of transport protein expression was observed, which points towards a somewhat higher expression of the

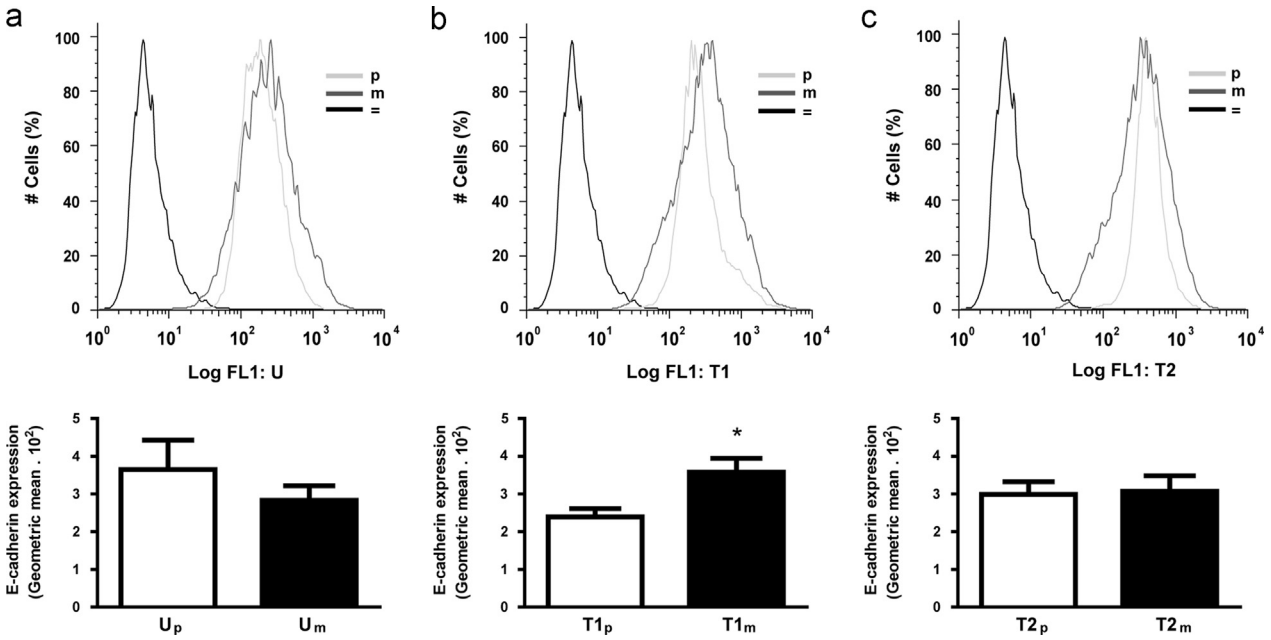

Fig. 3 – E-cadherin expression in proliferating and matured ciPTEC. (a–c) Representative E-cadherin flowcytometer histograms (FL1/Alexa 488 signal – Log scale) were shown in the upper panel of proliferating (light gray histogram) and matured (dark gray histogram) cells in the tested models. As a negative control (black histogram) ciPTEC were treated according to the protocol but the first antibody incubation step was excluded. (b; lower panel) Upon maturation (black bar), ciPTEC-T1 showed a higher geometric mean as compared to proliferating ciPTEC-T1 (white bar). (a–c; upper panel) Nevertheless, upon maturation all models clearly showed a more heterogeneous population regarding E-cadherin expression compared to proliferating cells. Data are shown as mean ± S.E.M. of three independent experiments. * = $p < 0.05$ using an unpaired *t* test.

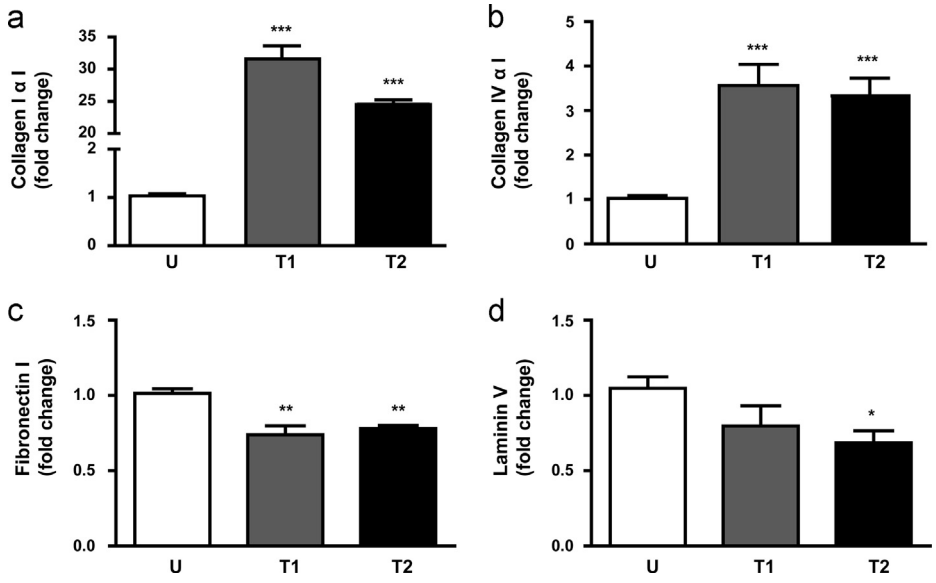

Fig. 4 – Expression of extracellular matrix genes in matured ciPTEC models. (a and b) Both cell lines derived from kidney tissue showed a higher gene expression of collagen I α1 (a) and -IV α1 (b) compared to ciPTEC-U. (c) In ciPTEC-T1 and -T2, a lower gene expression of fibronectin I was observed compared to ciPTEC-U. (d) In ciPTEC-T2, a lower gene expression of laminin 5 was observed compared to ciPTEC-U. Expression levels were corrected for corresponding GAPDH mRNA levels and data are expressed as fold change and compared to ciPTEC-U. Data are presented as means of three independent experiments ± S.E.M. * = $p < 0.05$, ** = $p < 0.01$, *** = $p < 0.001$, using an ANOVA analysis followed by Dunnett's multiple comparison test.

investigated transporters as compared to the corresponding proliferating cells (Fig. 6). The expression levels between the different cell lines in their proliferating or matured state was not significantly different.

Functional transport in ciPTEC

To functionally characterize OCTs, we used a recently established assay based on the uptake of the fluorescent marker substrate

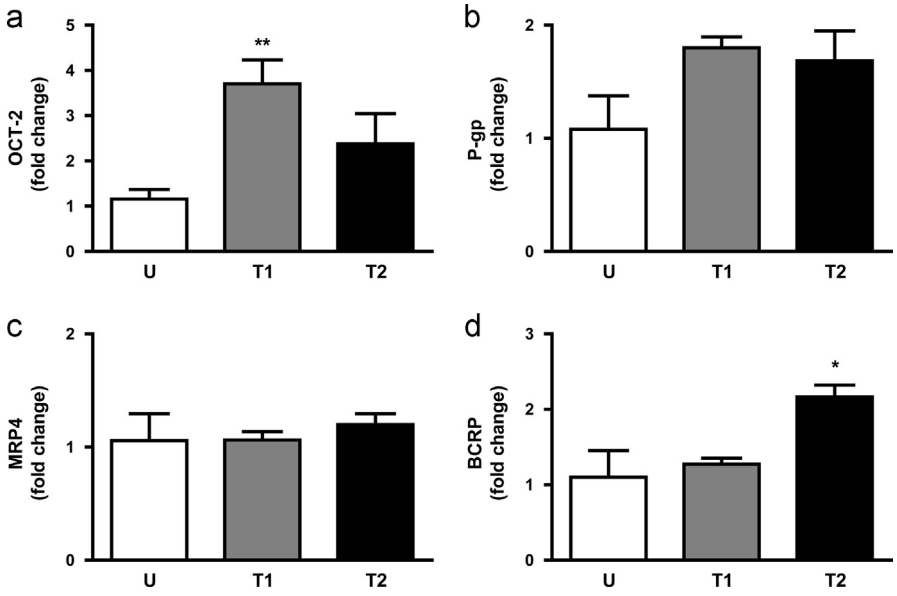

Fig. 5 – Expression of proximal tubular specific transporters in matured ciPTEC models. (a) In ciPTEC-T1 a higher OCT-2 gene expression was observed compared to ciPTEC-U. (b and c) No significant differences in P-gp (b) and MRP4 (c) gene expressions were observed between the three cell lines. (d) In ciPTEC-T2 a higher BCRP gene expression was observed compared to ciPTEC-U. Expression levels were corrected for corresponding GAPDH mRNA levels and data were expressed as fold change and compared to ciPTEC-U. Data are presented as means of three independent experiments ± S.E.M. * = $p < 0.05$, ** = $p < 0.01$, using an ANOVA analysis followed by Dunnett's multiple comparison test.

ASP^+ in ciPTEC suspensions [26]. All three cell lines showed a clear ASP^+ uptake, which was sensitive to inhibition by TPA ($p < 0.001$), indicating active OCTs present in each ciPTEC model (Fig. 7a). To compare the activity between the cell lines, the net ASP^+ uptake was calculated, which was higher in ciPTEC-U (80 ± 8 RFU/1,000 cells) compared to ciPTEC-T1 (53 ± 2 RFU/1,000 cells; $p < 0.05$), whereas no difference was observed between ciPTEC-U and -T2 (net transport 71 ± 5 RFU/1,000 cells).

The functional expression of P-gp was examined by measuring intracellular accumulation of calcein in matured cells, as described earlier [35]. The inhibitor PSC833 was used to obtain accumulated intracellular fluorescent signals due to P-gp inhibition (Fig. 7b). An increased accumulation was determined in all ciPTEC cell lines ($p < 0.001$), indicating functional P-gp present in each ciPTEC model. To compare the activity between the cell lines, the net calcein fluorescence was determined and a clearly higher calcein accumulation was observed in both cell lines established from kidney tissue (ciPTEC-T1 7.3 ± 0.6 RFU · 10^3 · mg protein^{-1} · cm^{-2}; $p < 0.01$ and ciPTEC-T2 7.2 ± 0.4 RFU · 10^3 · mg protein^{-1} cm^{-2}; $p < 0.05$) compared to ciPTEC-U (5.3 ± 0.4 RFU · 10^3 · mg protein^{-1} · cm^{-2}).

The functional properties of BCRP and MRP4 were investigated by exposing matured ciPTEC models to kynurenic acid (Fig. 7c). The compounds MK571 in combination with KO143 were used as MRP4 and BCRP inhibitors, respectively [37,38]. A higher accumulation was observed in ciPTEC-U in the presence of inhibitors ($p < 0.05$). In both tissue derived cell lines, kynurenic acid accumulation was slightly increased in presence of the inhibitors but this effect was not significant. To investigate and compare the BCRP and MRP4 properties between matured ciPTEC models, the net accumulation of kynurenic acid was calculated and compared to ciPTEC-U (1.1 ± 0.4 pmol · mg protein^{-1} · cm^{-2}), but no differences were observed (ciPTEC-T1 0.7 ± 0.6 pmol · mg protein^{-1} · cm^{-2}, ciPTEC-T2 0.9 ± 0.3 pmol · mg protein^{-1} · cm^{-2}).

In addition to uremic toxin excretion, proximal tubule cells also play an important role in renal reabsorption processes. Wilmer et al. [44] and Gorvin et al. [12] previously reported on the presence of megalin in ciPTEC-U and specific megalin mediated albumin endocytosis was confirmed with the megalin-blocker recombinant receptor-associated protein (RAP). The temperature-sensitive reabsorption of albumin was investigated in the three cell lines (Fig. 8a; upper panel). The reabsorption was similar in ciPTEC-T1 as compared to ciPTEC-U, whereas ciPTEC-T2 demonstrated a higher uptake of albumin (Fig. 8a; lower panel; $p < 0.001$).

Another PTEC feature concerns sodium-dependent phosphate re-absorption, mediated via NaPi-IIa and NaPi-IIc and driven by the free energy provided by the electrochemical gradient for Na^+. The transporters are located at the luminal side of proximal tubular cells [16]. The mRNA expression of both phosphate transporters was confirmed in proliferating and matured cells (Fig. S3) and uptake in matured ciPTEC-U, -T1 and -T2 was studied (Fig. 8b). Sodium-dependent phosphate uptake was found to be lower in ciPTEC-T1 and -T2 ($p < 0.01$) as compared to ciPTEC-U. In proliferating cells sodium-dependent phosphate uptake was determined as well (Fig. S4), furthermore, the uptake was clearly higher in matured cells as compared to proliferating cells.

Discussion

In this study, human conditionally immortalized proximal tubular epithelial cell lines were successfully developed from kidney tissue. Characterization of the newly established human cell lines

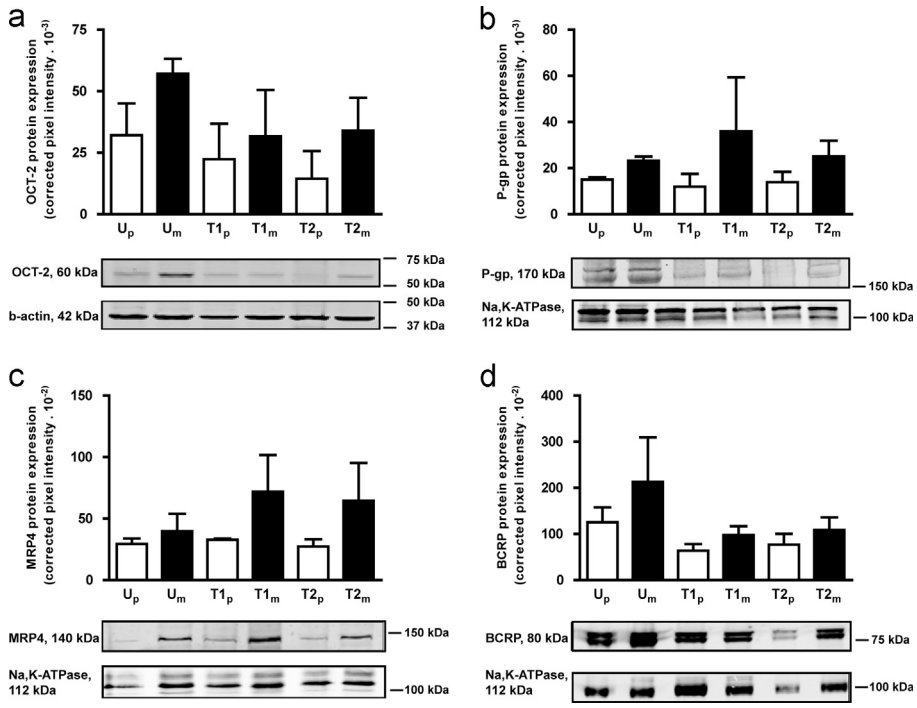

Fig. 6 – Protein expression of OCT-2, P-gp, MRP4 and BCRP in membrane fractions of ciPTEC-U, -T1 and -T2. (a–d) Although not significant, all matured (black bars) ciPTEC showed a slight increased OCT-2 (a), P-gp (b), MRP4 (c) and BCRP (d) expression compared to proliferating (white bars) ciPTEC. Signal intensities were corrected for the corresponding reference protein, which was used as a loading control and expression was analyzed semi-quantitative by measuring pixel intensity. Note that due to Western blot conditions Na,K-ATPase appears in multiple bands (b and c). Hence, for semi-quantification the intensity between 100 and 120 kDa was used as a reference. To semi-quantify the OCT-2 expression, β-actin was used as a reference protein since the molecular mass of β-actin (42 kDa) is more within the mass range of OCT-2 (60 kDa) than Na,K-ATPase (112 kDa). The blots presented are representative for protein expression in the ciPTEC models. Data are presented as means of three independent experiments ± S.E.M and statistical analysis was performed using an ANOVA analysis followed by Dunnett's multiple comparison test.

and comparison with a cell line isolated from urine revealed that cells from both sources comparably maintain renal physiological properties. A broad range of parameters was endogenously present in the three cell lines, including the ability to form tight monolayers, ECM deposition and diverse transport activities. On a functional level, the cells isolated from kidney tissue were able to compete with the previously characterized cell line isolated from urine (ciPTEC-U), while collagen I and -IV α1 gene expression was more pronounced in cells derived from renal tissue samples.

To maintain homeostatic cell numbers in the epithelium, live cell extrusion can take place in epithelial cells into the tubular lumen [28]. Although viable cells can be exfoliated in urine, their release might be the result of reduced capability to excrete ECM proteins as demonstrated in this study. The cell lines derived from kidney tissue showed a more pronounced endogenous expression of collagen I and -IV α1 as compared to ciPTEC-U, and monolayer formation of the urine derived cell line was clearly improved by collagen IV coating of culture material. These findings suggest that despite the more abundant gene expression of both fibronectin I and laminin 5 in matured ciPTEC-U, lower levels of essential collagen I and IV α1 expression prevents these cells from developing tight monolayers. In the kidney, the ECM proteins play an important role in intracellular signaling including cell proliferation, survival and migration as well in repair [42,43]. Therefore, it could be argued, that ciPTEC-U has limited properties with respect to ECM and related signaling functions. However, based on the functional data and E-cadherin expression obtained in this study, ciPTEC-U nicely competes with the cells originally derived from kidney tissue. Functionally active OCT-2, P-gp, MRP4 and BCRP mediated transport was detected in all models tested, and no superior cell line with respect to the activity of the investigated transport proteins was identified. Furthermore, active albumin reabsorption and sodium-dependent phosphate uptake were measured in ciPTEC-U, ciPTEC-T1 and -T2, with only small variations between the cell lines.

Gene and protein expressions of OCT-2, P-gp, MRP4 and BCRP transporters confirmed the endogenous presence of these proteins in ciPTEC-U, -T1 and -T2. The small differences between the three cell models most likely reflect the biovariability. Importantly, the ciPTEC models showed an extensive endogenous expression profile upon maturation, emphasizing the differentiation capacity of these human PTEC lines by immortalization using the temperature sensitive SV40 tsA58 antigen. In the panel of transporters tested, only BCRP was less abundantly present in matured cells as compared to proliferating cells (Supplementary Fig. S2d). This observation can be explained by the role of this efflux pump in kidney regeneration where it has a distinct function during cell development and a less prominent expression upon maturation [45].

Interestingly, although the gene expression levels of the four transporters investigated were lower in matured ciPTEC-U as

compared to matured ciPTEC-T1 and -T2, their protein expressions and activities were almost equal in the three models. These observations might reflect differences in post-transcriptional or -translational regulation of the transport proteins. The first step from mRNA to protein can be influenced by epigenetic alterations in signaling molecules, such as Wnt proteins and DNA-binding factors which play a key role in proximal tubular cell development [46]. The differences in the next step from inactive to a functional and active transport protein can possibly be influenced by an altered activity of kinases and/or phosphatases responsible for phosphorylation and dephosphorylation, respectively [47]. Future research directed towards these pathways should reveal how the four transporters can be modulated in the cell lines.

Robust transport activity was undoubtedly proven for OCTs and P-gp, while the activity of MRP4 and BCRP was less pronounced with the assay used. For the latter transporters the combined substrate kynurenic acid [24] was used in combination with inhibitors for MRP4 and BCRP. A plausible explanation for the limited effect of both inhibitors on kynurenic acid accumulation may be the absence of a specific uptake transporter for kynurenic acid. The uremic metabolite was proven to be an equally potent substrate for the basolaterally expressed organic anion transporters 1 (OAT-1) and -3 (OAT-3) [48]. OAT1 and OAT3 form important influx transporters in proximal tubular cells and determinants in the excretion of a variety of organic anions, including waste products from normal metabolism and drugs [49,50]. Unfortunately, these transporters are absent on gene, protein and functional levels in the immortalized cell lines isolated from both urine and kidney tissue (data not shown). Although the expression of OATs has been observed in primary proximal tubular cells [51], the levels decrease dramatically during the first days of culturing and are lost after cell passaging (unpublished observations). This phenomenon has already been described in 1990 by Miller [52] and has, as of yet, not been solved. Stable expression of these OATs in renal cell lines may not only be of importance for studying regenerative nephrology, but may also be of great value for drug development in pharmaceutical industry. Next to the OAT transporters, OATP4C1 is another known anion uptake transporter expressed at the basal membrane of proximal tubule cells [53]. The gene expression was studied in these cell lines and the expression of OATP4C1 was confirmed in matured cells (an average $C(t)$ value of 27.2 ± 0.1 was detected). Assays to demonstrate the functionality of this transporter are in progress. To study the role of transporters in disposition of new pharmaceutical entities and to identify potential drug-drug interactions, a need exists for human models

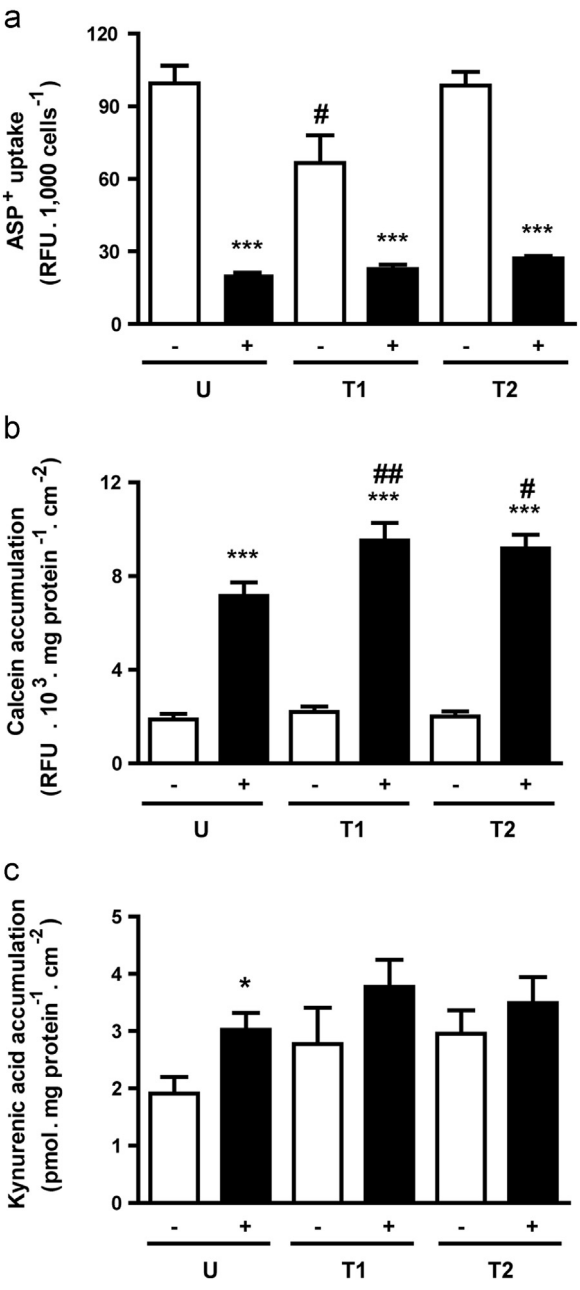

Fig. 7 – Functional in- and efflux proteins in matured ciPTEC. (a) OCT mediated ASP^+ uptake was measured in matured ciPTEC in the presence (black bars) or absence (white bars) of an inhibitor, TPA (5 mM). All ciPTEC models showed ASP^+ uptake which was sensitive to inhibition by TPA, confirming specific OCT activity. In ciPTEC-T1 the net ASP^+ uptake (values without inhibitor subtracted from values in presence of TPA) was lower compared to ciPTEC-U. (b) The P-gp activity in matured ciPTEC was measured in the presence (black bars) or absence (white bars) of a P-gp inhibitor, PSC833. An increased accumulation of calcein was observed in all cell lines in the presence of the P-gp inhibitor. Moreover, in ciPTEC-T1 and -T2 the net calcein accumulation (values without inhibitor subtracted from values in presence of PSC833) was higher as compared to ciPTEC-U. (c) The activity of MRP4 and BCRP in matured ciPTEC was detected in the presence (black bars) or absence (white bars) of the inhibitors, MK571 and KO143. A significant increased accumulation of kynurenic acid was observed in ciPTEC-U in the presence of the inhibitors. Although not significant, a slightly increased accumulation of kynurenic acid was detected in ciPTEC-T1 and -T2. The net kynurenic acid accumulation (values without subtracted from values in presence of both inhibitors) showed no differences between the cell lines. Data are presented as means of three independent experiments ± S.E.M. *$= p < 0.05$, *$= p < 0.001$ compared to data in the absence of inhibitors per cell line, using an unpaired t test. #$= p < 0.05$, ##$= p < 0.01$ compared to net activity in ciPTEC-U, using an ANOVA analysis followed by Dunnett's multiple comparison test.**

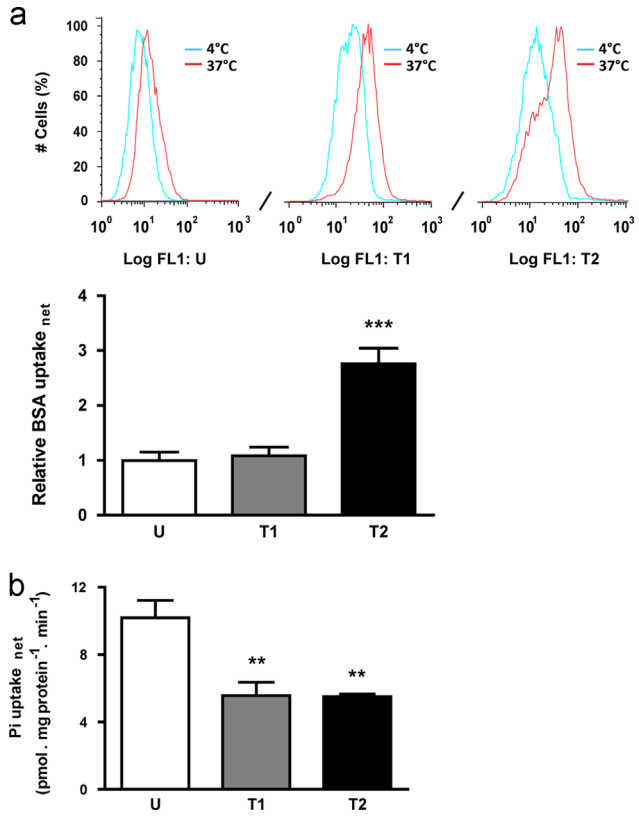

Fig. 8 – Essential reabsorption of albumin and phosphate in PTEC. (a; upper panel) The albumin reabsorption was detected in matured cells incubated at 4 °C (blue histogram) and 37 °C (red histogram) during experimental processing (15,000 cells counted). The signal intensities obtained at 37 °C clearly showed specific reabsorption in each model. (a; lower panel) The net albumin reabsorption was determined in matured ciPTEC and calculated by subtracting a-specific reabsorption data detected at 4 °C from values determined at 37 °C. A significantly increased albumin reabsorption was observed in ciPTEC-T2 as compared to ciPTEC-U. (b) The net sodium-dependent phosphate uptake was investigated in matured ciPTEC and calculated by subtracting sodium-independent uptake data from the uptake determined in presence of sodium. A significantly increased sodium-dependent phosphate uptake was detected in ciPTEC-U compared to ciPTEC-T1 and T2. Data are shown as mean ± S.E.M. of three independent experiments. ** = $p < 0.01$, *** = $p < 0.001$, using one-way ANOVA analysis followed by Dunnett's multiple comparison test.

predictive for renal drug handling [44,54,55]. Future research will be directed to further develop and optimize such models.

Next to the functional basal uptake and apical efflux transport, active albumin reabsorption and sodium-dependent phosphate uptake are essential processes occurring in human PTEC. Both mechanisms were detected in our ciPTEC models, although differences were observed between the cell lines. These findings underline the heterogeneity with respect to their endocytosis-mediated albumin uptake via megalin, and NaPi-IIa and -IIc mediated sodium-dependent phosphate uptake. As described before, post-transcriptional and -translational differences in these cell lines might explain the observed variability.

Isolating functional renal epithelial cells from human urine and applying conditional immortalization strategies could be a valuable tool in tissue engineering for personalized medicine in patients suffering from renal disorders, e.g. in development of a bioartificial kidney device [12]. Indications exist that residual renal function in CKD represents urine produced by tubular secretion rather than glomerular filtration [56]. Residual renal function is a predictor of survival in patients treated with dialysis [57]. Retaining or improving active tubular secretion processes may have profound effects on clinical outcome of CKD patients and the use bioartificial devices may be a good treatment alternative for this patient population [12]. However, the amount and the quality of functional cells in urine originating from these patients might be questionable. In this study, cells from healthy volunteers were transduced using hTERT in combination with the temperature sensitive SV40t gene [19,31]. Although Wieser et al. [58] previously used a single transduction of hTERT only to immortalize primary renal cells, in our laboratory this method did not lead to successful immortalization and hTERT only transductions resulted in dysmorphic cells. A great advantage of using the combined immortalization strategy is that cells can remain in their proliferating state at 33°C, thereby providing an unlimited cell source. Maturation can be initiated by transferring cells to 37 °C, upon which the expression of SV40t in ciPTEC decreases [19] and expression levels of PTEC specific proteins adequately increases (Supplementary Figs. S1–S3). These findings support their suitability for studying regenerative nephrology. However, the oncogene transductions used require stringent biological safety regulation (e.g. filters absorbing eventually disrupted cells) before implementing in any clinical application, which is the focus of ongoing research and obviously a thorough risk assessment is needed The use of serum-free culture conditions might be favorable to reduce a possible host immune response. However, culturing the ciPTEC models using serum-free medium for more than 24 h induces epithelial-to-mesenchymal transition (EMT) and results in a loss of PTEC-specific characteristics (data not shown). Serum-replacement compounds might be an appropriate alternative, but to this end comprehensive research is required to study the possible effect in these PTEC models prior to implementation.

In conclusion, the human renal lines established from urine and kidney tissue display a comparable variety of functional PTEC specific transporters with maintained reabsorption mechanisms. Interestingly, a different ECM profile was observed in the cell lines isolated from kidney tissue as compared to the cell line isolated from cells exfoliated in urine. The cell models presented here could serve as valuable tools to study proximal tubule physiology and pharmacology. Furthermore, the availability of inexhaustible sources of functional human proximal tubule epithelial cells could allow for further development and up scaling of bioartificial kidney devices.

Ethical standards

The experiments described in this article comply with the current laws of the country in which they were performed (the Netherlands).

Conflict of interest

The authors declare that they have no conflict of interest.

Acknowledgment

This research forms part of the Project P3.01 BioKid of the research program of the BioMedical Materials institute, co-funded by the Dutch Ministry of Economic Affairs. The financial contribution of the Dutch Kidney Foundation is gratefully acknowledged (IK08.03 and KJPB 11.0023) and the Netherlands Institute for Regenerative Medicine (NIRM, Grant no. FES0908) and the Netherlands Organization for Scientific Research (016.130.668).

Appendix A. Supporting information

Supplementary data associated with this article can be found in the online version at http://dx.doi.org/10.1016/j.yexcr.2014.02.011.

REFERENCES

[1] C.S. Fox, K. Matsushita, M. Woodward, H.J. Bilo, J. Chalmers, H.J. Heerspink, et al., Associations of kidney disease measures with mortality and end-stage renal disease in individuals with and without diabetes: a meta-analysis, Lancet 380 (2012) 1662.
[2] B.K. Mahmoodi, K. Matsushita, M. Woodward, P.J. Blankestijn, M. Cirillo, T. Ohkubo, et al., Associations of kidney disease measures with mortality and end-stage renal disease in individuals with and without hypertension: a meta-analysis, Lancet 380 (2012) 1649.
[3] C.G. Winearls, R.J. Glassock, Classification of chronic kidney disease in the elderly: pitfalls and errors, Nephron Clin. Pract. 119 (Suppl 1) (2011) c2.
[4] D.H. Krieter, A. Hackl, A. Rodriguez, L. Chenine, H.L. Moragues, H.D. Lemke, et al., Protein-bound uraemic toxin removal in haemodialysis and post-dilution haemodiafiltration, Nephrol., Dial., Transplant.: Off. Publ. Eur. Dial. Transplant Assoc.—Eur. Renal Assoc. 25 (2010) 212.
[5] R. Vanholder, S. Van Laecke, G. Glorieux, What is new in uremic toxicity?, Pediatr. Nephrol. 23 (2008) 1211.
[6] R. Vanholder, R. De Smet, Pathophysiologic effects of uremic retention solutes, J. Am. Soc. Nephrol. 10 (1999) 1815.
[7] B.R. Morgan, H.N. Ibrahim, Long-term outcomes of kidney donors, Curr. Opin. Nephrol. Hypertens. 20 (2011) 605.
[8] R.A. Wolfe, V.B. Ashby, E.L. Milford, A.O. Ojo, R.E. Ettenger, L.Y. Agodoa, et al., Comparison of mortality in all patients on dialysis, patients on dialysis awaiting transplantation, and recipients of a first cadaveric transplant, N. Engl. J. Med. 341 (1999) 1725.
[9] M.A. Artz, J.M. Boots, G. Ligtenberg, J.I. Roodnat, M.H. Christiaans, P.F. Vos, et al., Conversion from cyclosporine to tacrolimus improves quality-of-life indices, renal graft function and cardiovascular risk profile, Am. J. Transplant.: Off. J. Am. Soc. Transplant. Am. Soc. Transplant Surg. 4 (2004) 937.
[10] E.J. Hoorn, S.B. Walsh, J.A. McCormick, A. Furstenberg, C.L. Yang, T. Roeschel, et al., The calcineurin inhibitor tacrolimus activates the renal sodium chloride cotransporter to cause hypertension, Nat. Med. 17 (2011) 1304.
[11] D.L. Segev, Innovative strategies in living donor kidney transplantation, Nat. Rev. Nephrol. 8 (2012) 332.
[12] H.D. Humes, D. Buffington, A.J. Westover, S. Roy, W.H. Fissell, The bioartificial kidney: current status and future promise, Pediatr. Nephrol. (2013).
[13] H. Koepsell, H. Endou, The SLC22 drug transporter family, Pflugers Arch.: Eur. J. Physiol. 447 (2004) 666.
[14] R. Masereeuw, F.G. Russel, Regulatory pathways for ATP-binding cassette transport proteins in kidney proximal tubules, AAPS J. 14 (2012) 883.
[15] N. Anzai, K. Ichida, P. Jutabha, T. Kimura, E. Babu, C.J. Jin, et al., Plasma urate level is directly regulated by a voltage-driven urate efflux transporter URATv1 (SLC2A9) in humans, J. Biol. Chem. 283 (2008) 26834.
[16] I.C. Forster, N. Hernando, J. Biber, H. Murer, Proximal tubular handling of phosphate: a molecular perspective, Kidney Int. 70 (2006) 1548.
[17] M. Gekle, Renal tubule albumin transport, Annu. Rev. Physiol. 67 (2005) 573.
[18] C.L. Triplitt, Understanding the kidneys' role in blood glucose regulation, Am. J. Managed Care 18 (2012) S11.
[19] M.J. Wilmer, M.A. Saleem, R. Masereeuw, L. Ni, T.J. van der Velden, F.G. Russel, et al., Novel conditionally immortalized human proximal tubule cell line expressing functional influx and efflux transporters, Cell Tissue Res. 339 (2010) 449.
[20] C.M. Gorvin, M.J. Wilmer, S.E. Piret, B. Harding, L.P. van den Heuvel, O. Wrong, et al., Receptor-mediated endocytosis and endosomal acidification is impaired in proximal tubule epithelial cells of Dent disease patients, Proc. Ntl. Acad. Sci. USA 110 (2013) 7014.
[21] D. Mekahli, E. Sammels, T. Luyten, K. Welkenhuyzen, L.P. van den Heuvel, E.N. Levtchenko, et al., Polycystin-1 and polycystin-2 are both required to amplify inositol-trisphosphate-induced Ca^{2+} release, Cell Calcium 51 (2012) 452.
[22] H.A. Mutsaers, M.J. Wilmer, D. Reijnders, J. Jansen, P.H. van den Broek, M. Forkink, et al., Uremic toxins inhibit renal metabolic capacity through interference with glucuronidation and mitochondrial respiration, Biochim. Biophys. Acta 1832 (2013) 142.
[23] M.J. Wilmer, L.A. Kluijtmans, T.J. van der Velden, P.H. Willems, P.G. Scheffer, R. Masereeuw, et al., Cysteamine restores glutathione redox status in cultured cystinotic proximal tubular epithelial cells, Biochim. Biophys. Acta 1812 (2011) 643.
[24] A.C. Dankers, H.A. Mutsaers, H.B. Dijkman, L.P. van den Heuvel, J.G. Hoenderop, F.C. Sweep, et al., Hyperuricemia influences tryptophan metabolism via inhibition of multidrug resistance protein 4 (MRP4) and breast cancer resistance protein (BCRP), Biochim. Biophys. Acta (2013).
[25] H.A. Mutsaers, L.P. van den Heuvel, L.H. Ringens, A.C. Dankers, F.G. Russel, J.F. Wetzels, et al., Uremic toxins inhibit transport by breast cancer resistance protein and multidrug resistance protein 4 at clinically relevant concentrations, PLoS One 6 (2011) e18438.
[26] C.M. Schophuizen, M.J. Wilmer, J. Jansen, L. Gustavsson, C. Hilgendorf, J.G. Hoenderop, et al., Cationic uremic toxins affect human renal proximal tubule cell functioning through interaction with the organic cation transporter, Pflugers Arch.: Eur. J. Physiol. 465 (2013) 1701.
[27] J. Rosenblatt, M.C. Raff, L.P. Cramer, An epithelial cell destined for apoptosis signals its neighbors to extrude it by an actin- and myosin-dependent mechanism, Curr. Biol. 11 (2001) 1847.
[28] G.T. Eisenhoffer, P.D. Loftus, M. Yoshigi, H. Otsuna, C.B. Chien, P.A. Morcos, et al., Crowding induces live cell extrusion to maintain homeostatic cell numbers in epithelia, Nature 484 (2012) 546.
[29] P.A. van Setten, V.W. van Hinsbergh, T.J. van der Velden, N.C. van de Kar, M. Vermeer, J.D. Mahan, et al., Effects of TNF alpha on verocytotoxin cytotoxicity in purified human glomerular microvascular endothelial cells, Kidney Int. 51 (1997) 1245.
[30] F.A. Reubsaet, J.H. Veerkamp, L.A. Monnens, Sulfated glycosaminoglycan content of glomerular and tubular basement membranes of individuals of different ages, Nephron 41 (1985) 344.

[31] M.A. Saleem, M.J. O'Hare, J. Reiser, R.J. Coward, C.D. Inward, T. Farren, et al., A conditionally immortalized human podocyte cell line demonstrating nephrin and podocin expression, J. Am. Soc. Nephrol. 13 (2002) 630.
[32] C.E. Hills, T. Jin, E. Siamantouras, I.K. Liu, K.P. Jefferson, P.E. Squires, 'Special k' and a loss of cell-to-cell adhesion in proximal tubule-derived epithelial cells: modulation of the adherens junction complex by ketamine, PLoS One 8 (2013)e71819 8 (2013).
[33] R.A. van Aubel, P.H. Smeets, J.G. Peters, R.J. Bindels, F.G. Russel, The MRP4/ABCC4 gene encodes a novel apical organic anion transporter in human kidney proximal tubules: putative efflux pump for urinary cAMP and cGMP, J. Am.Soc. Nephrol. 13 (2002) 595.
[34] J.B. Koenderink, S. Geibel, E. Grabsch, J.J. De Pont, E. Bamberg, T. Friedrich, Electrophysiological analysis of the mutated Na,K-ATPase cation binding pocket, J Biol. Chem. 278 (2003) 51213.
[35] F.M. van de Water, J.M. Boleij, J.G. Peters, F.G. Russel, R. Masereeuw, Characterization of P-glycoprotein and multidrug resistance proteins in rat kidney and intestinal cell lines, Eur. J. Pharm. Sci.: Off. J. Eur. Fed. Pharm. Sci. 30 (2007) 36.
[36] M. Huls, C.D. Brown, A.S. Windass, R. Sayer, J.J. van den Heuvel, S. Heemskerk, et al., The breast cancer resistance protein transporter ABCG2 is expressed in the human kidney proximal tubule apical membrane, Kidney Int. 73 (2008) 220.
[37] J.D. Allen, A. van Loevezijn, J.M. Lakhai, M. van der Valk, O. van Tellingen, G. Reid, et al., Potent and specific inhibition of the breast cancer resistance protein multidrug transporter in vitro and in mouse intestine by a novel analogue of fumitremorgin C, Mol. Cancer Ther. 1 (2002) 417.
[38] A.K. Luders, R. Saborowski, U. Bickmeyer, Inhibition of multidrug/xenobiotic resistance transporter by MK571 improves dye (Fura 2) accumulation in crustacean tissues from lobster, shrimp, and isopod, Comp. Biochem. Physiol. Toxicol. Pharmacol.: CBP 150 (2009) 368.
[39] K. Malmstrom, G. Stange, H. Murer, Intracellular cascades in the parathyroid-hormone-dependent regulation of Na+/phosphate cotransport in OK cells, Biochem. J. 251 (1988) 207.
[40] A. Kirk, S. Campbell, P. Bass, J. Mason, J. Collins, Differential expression of claudin tight junction proteins in the human cortical nephron, Nephrol., Dial., Transplant.: Off. Publ. Eur. Dial. Transplant Assoc.—Eur. Renal Assoc. 25 (2010) 2107.
[41] O. Kwon, W.J. Nelson, R. Sibley, P. Huie, J.D. Scandling, D. Dafoe, et al., Backleak, tight junctions, and cell–cell adhesion in postischemic injury to the renal allograft, J. Clin. Invest. 101 (1998) 2054.
[42] P.A. Nony, R.G. Schnellmann, Interactions between collagen IV and collagen-binding integrins in renal cell repair after sublethal injury, Mol. Pharmacol. 60 (2001) 1226.
[43] A. Pozzi, R. Zent, Integrins in kidney disease, J. Am. Soc. Nephrol. (2013).
[44] K.M. Giacomini, S.M. Huang, Transporters in drug development and clinical pharmacology, Clin. Pharmacol. Ther. 94 (2013) 3.
[45] M. Huls, J.P. Schoeber, C.M. Verfaillie, A. Luttun, F. Ulloa-Montoya, A.L. Menke, et al., Deficiency of either P-glycoprotein or breast cancer resistance protein protect against acute kidney injury, Cell Transplant. 19 (2010) 1195.
[46] R. Woroniecki, A.B. Gaikwad, K. Susztak, Fetal environment, epigenetics, and pediatric renal disease, Pediatr. Nephrol. 26 (2011) 705.
[47] T. Terabayashi, M. Sakaguchi, K. Shinmyozu, T. Ohshima, A. Johjima, T. Ogura, et al., Phosphorylation of Kif26b promotes its polyubiquitination and subsequent proteasomal degradation during kidney development, PLoS One 7 (2012)e39714 7 (2012).
[48] Y. Uwai, H. Honjo, K. Iwamoto, Interaction and transport of kynurenic acid via human organic anion transporters hOAT1 and hOAT3, Pharmacol. Res.: Off. J. Italian Pharmacol. Soc. 65 (2012) 254.
[49] Y. Hagos, G. Burckhardt, B.C. Burckhardt, Human organic anion transporter OAT1 is not responsible for glutathione transport but mediates transport of glutamate derivatives, Am. J. Physiol. Renal Physiol. 304 (2013) F403.
[50] L. Wang, D.H. Sweet, Interaction of natural dietary and herbal anionic compounds and flavonoids with human organic anion transporters 1 (SLC22A6), 3 (SLC22A8), and 4 (SLC22A11), Evid.-Based Complementary Altern. Med.: eCAM 2013 (2013) 612527.
[51] C.D. Brown, R. Sayer, A.S. Windass, I.S. Haslam, M.E. De Broe, P.C. D'Haese, et al., Characterisation of human tubular cell monolayers as a model of proximal tubular xenobiotic handling, Toxicol. Appl. Pharmacol. 233 (2008) 428.
[52] J.H. Miller, Sodium-sensitive, probenecid-insensitive p-aminohippuric acid uptake in cultured renal proximal tubule cells of the rabbit, Proc. Soc. Exp. Biol. Med. Soc. Exp. Biol. Med. 199 (1992) 298.
[53] H. Yamaguchi, M. Sugie, M. Okada, T. Mikkaichi, T. Toyohara, T. Abe, et al., Transport of estrone 3-sulfate mediated by organic anion transporter OATP4C1: estrone 3-sulfate binds to the different recognition site for digoxin in OATP4C1, Drug Metab. Pharmacokinet. 25 (2010) 314.
[54] G. Ahlin, C. Hilgendorf, J. Karlsson, C.A. Szigyarto, M. Uhlen, P. Artursson, Endogenous gene and protein expression of drug-transporting proteins in cell lines routinely used in drug discovery programs, Drug Metab. Dispos.: Biol. Fate Chem. 37 (2009) 2275.
[55] S.E. Jenkinson, G.W. Chung, E. van Loon, N.S. Bakar, A.M. Dalzell, C.D. Brown, The limitations of renal epithelial cell line HK-2 as a model of drug transporter expression and function in the proximal tubule, Pflugers Arch.: Eur. J. Physiol. 464 (2012) 601.
[56] J. Lowenstein, The anglerfish and uremic toxins, FASEB J.: Off. Publ. Fed. Am. Soc. Exp. Biol. 25 (2011) 1781.
[57] I.O. Marquez, S. Tambra, F.Y. Luo, Y. Li, N.S. Plummer, T.H. Hostetter, et al., Contribution of residual function to removal of protein-bound solutes in hemodialysis, Clin. J. Am. Soc. Nephrol. 6 (2011) 290.
[58] M. Wieser, G. Stadler, P. Jennings, B. Streubel, W. Pfaller, P. Ambros, et al., hTERT Alone immortalizes epithelial cells of renal proximal tubules without changing their functional characteristics, Am. J. Physiol. Renal Physiol. 295 (2008) F1365.